

# CT Fractional Flow Reserve for the Diagnosis of Myocardial Bridging-Related Ischemia: A Study Using Dynamic CT Myocardial Perfusion Imaging as a Reference Standard

Yarong Yu<sup>1\*</sup>, Lihua Yu<sup>1\*</sup>, Xu Dai<sup>1</sup>, Jiayin Zhang<sup>2</sup>

<sup>1</sup>Institute of Diagnostic and Interventional Radiology, Shanghai Jiao Tong University Affiliated Sixth People's Hospital, Shanghai, China;

<sup>2</sup>Department of Radiology, Shanghai General Hospital, Shanghai Jiao Tong University School of Medicine, Shanghai, China

**Objective:** To investigate the diagnostic performance of CT fractional flow reserve (CT-FFR) for myocardial bridging-related ischemia using dynamic CT myocardial perfusion imaging (CT-MPI) as a reference standard.

**Materials and Methods:** Dynamic CT-MPI and coronary CT angiography (CCTA) data obtained from 498 symptomatic patients were retrospectively reviewed. Seventy-five patients (mean age  $\pm$  standard deviation,  $62.7 \pm 13.2$  years; 48 males) who showed myocardial bridging in the left anterior descending artery without concomitant obstructive stenosis on the imaging were included. The change in CT-FFR across myocardial bridging ( $\Delta$ CT-FFR, defined as the difference in CT-FFR values between the proximal and distal ends of the myocardial bridging) in different cardiac phases, as well as other anatomical parameters, were measured to evaluate their performance for diagnosing myocardial bridging-related myocardial ischemia using dynamic CT-MPI as the reference standard (myocardial blood flow  $< 100$  mL/100 mL/min or myocardial blood flow ratio  $\leq 0.8$ ).

**Results:**  $\Delta$ CT-FFR<sub>systolic</sub> ( $\Delta$ CT-FFR calculated in the best systolic phase) was higher in patients with vs. without myocardial bridging-related myocardial ischemia (median [interquartile range],  $0.12 [0.08-0.17]$  vs.  $0.04 [0.01-0.07]$ ,  $p < 0.001$ ), while CT-FFR<sub>systolic</sub> (CT-FFR distal to the myocardial bridging calculated in the best systolic phase) was lower ( $0.85 [0.81-0.89]$  vs.  $0.91 [0.88-0.96]$ ,  $p = 0.043$ ). In contrast,  $\Delta$ CT-FFR<sub>diastolic</sub> ( $\Delta$ CT-FFR calculated in the best diastolic phase) and CT-FFR<sub>diastolic</sub> (CT-FFR distal to the myocardial bridging calculated in the best diastolic phase) did not differ significantly. Receiver operating characteristic curve analysis showed that  $\Delta$ CT-FFR<sub>systolic</sub> had largest area under the curve ( $0.822$ ; 95% confidence interval,  $0.717-0.901$ ) for identifying myocardial bridging-related ischemia.  $\Delta$ CT-FFR<sub>systolic</sub> had the highest sensitivity (91.7%) and negative predictive value (NPV) (97.8%).  $\Delta$ CT-FFR<sub>diastolic</sub> had the highest specificity (85.7%) for diagnosing myocardial bridging-related ischemia. The positive predictive values of all CT-related parameters were low.

**Conclusion:**  $\Delta$ CT-FFR<sub>systolic</sub> reliably excluded myocardial bridging-related ischemia with high sensitivity and NPV. Myocardial bridging showing positive CT-FFR results requires further evaluation.

**Keywords:** Myocardial bridging; Fractional flow reserve; Myocardial perfusion imaging; Computed tomography; Myocardial blood flow

**Received:** January 13, 2021 **Revised:** June 27, 2021 **Accepted:** July 26, 2021

This study is supported by Medical Guidance Scientific Research Support Project of Shanghai Science and Technology Commission (Grant No. 19411965100) and Shanghai Municipal Education Commission-Gaofeng Clinical Medicine Grant Support (Grant No. 20161428).

\*These authors contributed equally to this work.

**Corresponding author:** Jiayin Zhang, MD, Department of Radiology, Shanghai General Hospital, Shanghai Jiao Tong University School of Medicine, #86 Wujin Rd, Shanghai 200080, China.

• E-mail: andrewssmu@msn.com

This is an Open Access article distributed under the terms of the Creative Commons Attribution Non-Commercial License (<https://creativecommons.org/licenses/by-nc/4.0>) which permits unrestricted non-commercial use, distribution, and reproduction in any medium, provided the original work is properly cited.

## INTRODUCTION

Myocardial bridging is a commonly encountered anomaly finding on coronary CT angiography (CCTA) [1-4]. It is defined as an epicardial segment of coronary artery tunneling through the myocardium and occurs almost exclusively in the middle portion of the left anterior descending artery (LAD) [5]. Although considered a benign form of coronary anomaly, myocardial bridging is potentially associated with various clinical conditions such as myocardial ischemia, acute coronary syndromes, coronary spasm, and even sudden cardiac death [6-8].

Detecting hemodynamically significant myocardial bridging (i.e., myocardial ischemia) is of clinical interest to guide proper treatment strategies [9]. Recently, machine learning (ML)-based CT-FFR has shown high diagnostic performance compared to invasive FFR for identifying functional ischemia in vessels with myocardial bridging [10]. However, the hemodynamics of myocardial bridging differ from those of fixed atherosclerotic stenosis owing to the dynamic compression and changing morphology across cardiac circles. CT-FFR or invasive FFR might be insufficient for the precise functional assessment of myocardial bridging [9]. Moreover, it remains unclear what cardiac phase (systolic or diastolic) used for CT-FFR simulation has better diagnostic performance to identify myocardial bridging with myocardial ischemia.

Dynamic CT myocardial perfusion imaging (CT-MPI) is an accurate quantitative method established for the diagnosis of myocardial ischemia with reference to magnetic resonance MPI, nuclear MPI, or invasive fractional flow reserve (FFR) [11-15]. The myocardial blood flow (MBF) derived from dynamic CT-MPI has been validated as an accurate parameter against MBF derived from microsphere measurement in large animal studies [16,17]. In addition, functional assessment of myocardial bridging by dynamic CT-MPI solely depends on the level of downstream myocardial perfusion, which is not affected by the complex fluid dynamics of the tunneled coronary segment and can reflect the actual hemodynamic status of myocardial bridging. Therefore, the current study investigated the diagnostic performance of CT-FFR derived from different cardiac phases for evaluating myocardial bridging-related ischemia using dynamic CT-MPI findings as a reference standard.

## MATERIALS AND METHODS

### Patient Population

The hospital ethics committee approved this retrospective study (2020-104) and waived the requirement for informed patient consent. Between January 1, 2017, and June 30, 2020, 498 consecutive patients with stable angina and intermediate-to-high pretest probability of obstructive coronary artery disease (CAD) were referred for dynamic CT-MPI + CCTA. All data were reviewed, and patients were retrospectively included if myocardial bridging was detected on dynamic CT-MPI + CCTA. The exclusion criteria were as follows: 1) patients with concomitant obstructive coronary stenosis (defined as stenosis diameter  $\geq$  50%) on the myocardial bridging vessel, 2) insufficient CCTA image quality (either diastolic or systolic phase) for CT-FFR calculation, 3) significantly impaired dynamic CT-MPI image quality, 4) patients with a history of myocardial infarction or revascularization treatment on the myocardial bridging vessel, 5) patients with clinically suspected or confirmed cardiomyopathy, and 6) patients with clinically suspected or confirmed microvascular dysfunction. Of the 498 patients, 304 patients were initially excluded because of an absence of myocardial bridging. Another 119 patients were further excluded, as shown in Figure 1. Finally, 75 patients were included for further analysis (mean age  $\pm$  standard deviation [SD], 62.7  $\pm$  13.2 years, 48 males).

### Dynamic CT-MPI + CCTA Acquisition

All patients were scanned by third-generation dual-source CT (SOMATOM Force, Siemens Healthineers). An integrated protocol incorporating calcium score, dynamic CT-MPI, and CCTA, was used for acquisition. In brief, the calcium score was first calculated to determine the calcification burden of each pericardial vessel. Intravenous infusion of adenosine triphosphate at 160  $\mu$ g/kg/min was then administered for 3 minutes before initiating dynamic CT-MPI acquisition. Dynamic CT-MPI was acquired using a shuttle mode technique and started 4 seconds after beginning the contrast injection. Dynamic acquisition was set at the end-systolic phase (triggered 250 ms after the R wave in all patients) and scans were launched every second or third heart cycle according to the patients' heart rates. CARE kV and CARE dose 4D were used to reduce the radiation doses. The reference tube voltage and effective current were 80 kVp and 300 mA respectively.

Nitroglycerin was administered sublingually to all

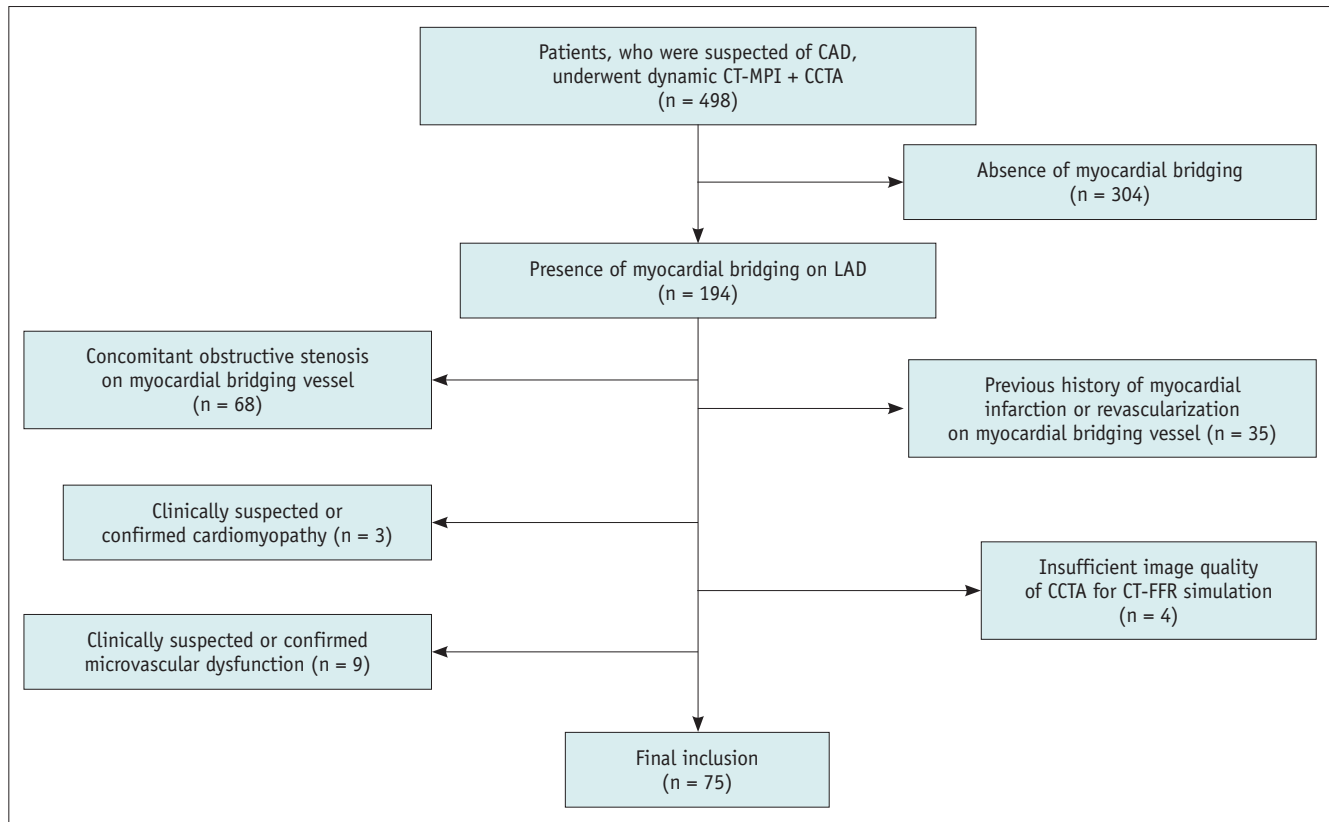


**Fig. 1. Flow chart of the inclusion and exclusion criteria.** CAD = coronary artery disease, CCTA = coronary CT angiography, FFR = fractional flow reserve, LAD = left anterior descending artery, MPI = myocardial perfusion imaging

subjects 5 minutes after dynamic CT-MPI. Prospective electrocardiogram-triggered sequential acquisition was performed in all participants for CCTA, with the acquisition window covering from 35% to 75% of the R-R interval. The detailed parameters of contrast medium injection, dynamic CT-MPI, and CCTA acquisition are provided in the Supplement (Supplementary Material).

### CCTA Assessment of Myocardial Bridging

CCTA data were reconstructed with a smooth kernel (Bv 40) and third-generation iterative reconstruction technique (strength 3, ADMIRE, Siemens Healthineers). The dataset with the best image quality from among all available phases was used for the morphological assessment of myocardial bridging.

Qualitative and quantitative analysis of myocardial bridging was performed on a commercially available workstation (Syngo.Via, VB20, Siemens Healthineers). Myocardial bridging was diagnosed at CCTA if a coronary segment was completely surrounded by the myocardium on cross-sectional images [4]. The quantitative measurements were manually made on the images of the best systolic

phase. The total myocardial bridging length was measured on curved planar reformation at the best projection view, from the entrance to exit points. The depth of the myocardial bridging was determined by measuring the maximal thickness of the overlying muscle on cross-sectional images. According to this thickness, myocardial bridging was further classified as superficial ( $\leq 2$  mm) or deep ( $> 2$  mm) [10]. One cardiovascular radiologist with 12 years of experience in cardiac imaging independently analyzed the above parameters.

### CT-FFR Calculation of Myocardial Bridging

This study applied an ML-based CT-FFR calculation algorithm (cFFR; version 3.0, Siemens Healthineers) that was previously investigated in myocardial bridging against invasive FFR [10]. In brief, this model was trained on a large database of synthesized coronary anatomies, where the reference values were computed using a computational fluid dynamics-based model [18]. Details regarding the training of this ML-based model and on-site processing are provided in the Supplement (Supplementary Material). One cardiovascular radiologist (with 12 years of experience

in cardiac imaging) analyzed the CT-FFR data. The lesion-specific CT-FFR was measured within 1 cm of the distal end of the myocardial bridging. The change in CT-FFR across myocardial bridging ( $\Delta$ CT-FFR) was also measured.  $\Delta$ CT-FFR was defined as the difference in CT-FFR values between the proximal and distal ends of the myocardial bridging [19]. Two sets of CCTA data (best systolic phase and best diastolic phase) were both used for CT-FFR calculation of myocardial bridging. Accordingly,  $\Delta$ CT-FFR<sub>systolic</sub> ( $\Delta$ CT-FFR calculated in the best systolic phase), CT-FFR<sub>systolic</sub> (CT-FFR distal to the myocardial bridging calculated in the best systolic phase) and  $\Delta$ CT-FFR<sub>diastolic</sub> ( $\Delta$ CT-FFR calculated in the best diastolic phase), CT-FFR<sub>diastolic</sub> (CT-FFR distal to the myocardial bridging calculated in the best diastolic phase) were recorded.

### Dynamic CT-MPI Analysis of Myocardial Bridging

The dataset of dynamic CT-MPI was reconstructed with a dedicated kernel (Qr36) for the reduction of iodine beam-hardening artifacts. A commercially available CT-MPI software package (Myocardial perfusion analysis, VPCT body, Siemens Healthineers) was used for further analysis. Motion correction was manually applied if breathing-related misregistration of the left ventricle was present. The quantification of MBF was performed using a hybrid deconvolution model, as previously reported [20].

One cardiovascular radiologist (with 12 years of experience in cardiac imaging) independently analyzed the MBF 2 weeks after CT-FFR analysis. The myocardial territories subtended by the myocardial bridging were individually determined according to the fusion images of coronary vasculature and the perfusion map. For measurement of absolute MBF, regions of interest (ROIs) were manually placed on a short-axis view on a segment base according to the 17-segment model with exclusion of the apical segment [21]. To measure the MBF of the myocardial bridging (MBF<sub>myocardial bridging</sub>), the ROI was drawn to cover the whole area of suspected perfusion defect within the myocardial bridging-subtended segments or the entire segment (with exclusion of the sub-endocardial and sub-epicardial area) when a perfusion defect was absent. The MBF of the reference segments (MBF<sub>reference</sub>) was defined as the segments supplied by the epicardial vessels without the presence of  $\geq 30\%$  stenosis, in which the hemodynamic status was considered insignificant [22]. Moreover, the MBF<sub>ratio</sub> was calculated as the MBF<sub>myocardial bridging</sub> vs. MBF<sub>reference</sub>. Based on the results from a previous dynamic CT-MPI

study, an absolute MBF of  $< 100$  mL/100 mL/min or an MBF<sub>ratio</sub> of  $\leq 0.8$  were considered to indicate the presence of myocardial ischemia [14,15]. Accordingly, myocardial bridging-related ischemia was defined as MBF<sub>myocardial bridging</sub> of  $< 100$  mL/100 mL/min or MBF<sub>ratio</sub> of  $\leq 0.8$ .

### Statistical Analysis

Statistical analyses were performed using MedCalc version 19.2 (MedCalc Software bvba). One-sample Kolmogorov-Smirnov tests were first used to check the assumption of normal distribution. Quantitative variables with normal distribution were expressed as means  $\pm$  SD, while variables that were not normally distributed were expressed as medians and interquartile range (IQR). Categorical variables were presented as numbers and percentages. Student's *t* test and Mann-Whitney U tests were used for normally and non-normally distributed data, respectively. Receiver operating characteristic (ROC) curve analyses were performed to calculate the areas under the curves (AUCs). The optimal cutoff values for various parameters were determined by the Youden index (maximum sum of sensitivity and specificity). Comparisons of AUCs of different parameters were conducted as described by DeLong et al. Sensitivity, specificity, negative predictive value (NPV), positive predictive value (PPV), and diagnostic accuracy were calculated. Intra-observer agreements of all parameters (two measurements at a 1-week interval) were tested by intraclass correlation coefficients. A two-tailed  $p < 0.05$  was considered statistically significant.

## RESULTS

### Patient Characteristics

The detailed clinical characteristics of the 75 study patients are shown in Table 1. The mean effective dose of radiation for dynamic CT-MPI + CCTA was 4.54 mSv (3.75–6.73 mSv) when using 0.014 as the conversion factor.

### CCTA and CT-FFR Features of Myocardial Bridging

The intra-observer agreement for the measurement of CT-derived parameters was good (Supplementary Table 1).

Conventional CCTA anatomical parameters, such as myocardial bridging length and depth, were compared between ischemic and non-ischemic myocardial bridging. For myocardial bridging causing myocardial ischemia, myocardial bridging length was not significantly longer, whereas superficial myocardial bridging was less frequently

observed (Table 2). In systole, the CT-FFR<sub>systolic</sub> values were significantly lower (median [IQR], 0.85 [0.81–0.89] vs. 0.91 [0.88–0.96],  $p = 0.043$ ) for ischemic myocardial bridging, while markedly higher  $\Delta$ CT-FFR<sub>systolic</sub> values (0.12 [0.08–0.17] vs. 0.04 [0.01–0.07],  $p < 0.001$ ) were observed (Table 2, Figs. 2, 3). In contrast, no significant differences were observed in CT-FFR<sub>diastolic</sub> (0.87 [0.84–0.91] vs. 0.91 [0.86–0.94],  $p = 0.548$ ) and  $\Delta$ CT-FFR<sub>diastolic</sub> (0.07 [0.03–0.10] vs. 0.03 [0.01–0.06],  $p = 0.096$ ) values between two groups (Table 2).

### Diagnostic Performance of CCTA and CT-FFR Parameters

The ROC analysis showed that  $\Delta$ CT-FFR<sub>systolic</sub> had the largest AUC (AUC = 0.822) among all parameters (Table 3, Fig. 4). The AUC of  $\Delta$ CT-FFR<sub>systolic</sub> was significantly larger than that of CT-FFR<sub>diastolic</sub> (AUC = 0.822 vs. AUC = 0.623,  $p = 0.029$ ). However, there was no statistical difference between the AUCs of  $\Delta$ CT-FFR<sub>systolic</sub> and  $\Delta$ CT-FFR<sub>diastolic</sub> (AUC = 0.822 vs. AUC = 0.652,  $p = 0.053$ ), as well as  $\Delta$ CT-FFR<sub>systolic</sub> and CT-FFR<sub>systolic</sub> (AUC = 0.822 vs. AUC = 0.733,  $p = 0.100$ ).  $\Delta$ CT-FFR<sub>systolic</sub> had the highest sensitivity (91.7%, 11/12) and NPV (97.8%, 44/45) whereas  $\Delta$ CT-FFR<sub>diastolic</sub> had the highest

**Table 1. Patient Characteristics**

	All Patients (n = 75)	Patients with Myocardial Bridging-Related Myocardial Ischemia (n = 12)	Patients without Myocardial Bridging-Related Myocardial Ischemia (n = 63)	P
Age, years*	62.7 ± 13.2	63.3 ± 13.4	62.1 ± 13.2	0.675
Male, number (%)	48 (64)	9 (75)	39 (62)	0.390
Risk factors, number (%)				
Diabetes mellitus	23 (31)	3 (25)	20 (32)	0.645
Hypertension	40 (53)	6 (50)	34 (54)	0.802
Dyslipidemia	17 (23)	3 (25)	14 (22)	0.834
Current smoking	13 (17)	3 (25)	10 (16)	0.447
CACS <sup>†</sup>	6.4 (0–145.4)	0.0 (0–16.6)	17.5 (0–168.5)	0.147
Clinical symptoms, number (%)				
Stable angina	34 (45)	7 (58)	27 (43)	0.327
Angina-equivalent symptoms	32 (43)	5 (42)	27 (43)	0.940
Chronic myocardial infarction <sup>‡</sup>	9 (12)	0 (0)	9 (14)	0.166
Pretest CAD probability, number (%) <sup>§</sup>				
15%–85%	57 (76)	9 (75)	48 (76)	0.930
≥ 86%	18 (24)	3 (25)	15 (24)	0.930

\*Data are mean ± standard deviation, <sup>†</sup>Data are the median, with the interquartile range in parentheses, <sup>‡</sup>Chronic myocardial infarction was not related to the left anterior descending artery territory, <sup>§</sup>Calculated by using the diamond and forrester chest pain prediction rule. CACS = coronary artery calcium scoring, CAD = coronary artery disease

**Table 2. CCTA and CT-FFR Features of Myocardial Bridging**

	All Patients (n = 75)	Patients with Myocardial Bridging-Related Myocardial Ischemia (n = 12)	Patients without Myocardial Bridging-Related Myocardial Ischemia (n = 63)	P
Myocardial bridging length, mm*	26.62 ± 13.08	32.03 ± 16.65	25.59 ± 12.18	0.119
Myocardial bridging depth, mm <sup>†</sup>	0.81 (0.44–1.42)	1.44 (0.75–2.84)	0.78 (0.27–1.30)	0.021
Superficial myocardial bridging, number (%)	61 (81)	7 (58)	54 (86)	0.027
Depth myocardial bridging, number (%)	14 (19)	5 (42)	9 (14)	0.027
CT-FFR <sub>systolic</sub> <sup>‡</sup>	0.90 (0.85–0.94)	0.85 (0.81–0.89)	0.91 (0.88–0.96)	0.043
$\Delta$ CT-FFR <sub>systolic</sub> <sup>‡</sup>	0.04 (0.01–0.09)	0.12 (0.08–0.17)	0.04 (0.01–0.07)	< 0.001
CT-FFR <sub>diastolic</sub> <sup>‡</sup>	0.91 (0.85–0.95)	0.87 (0.84–0.91)	0.91 (0.86–0.94)	0.548
$\Delta$ CT-FFR <sub>diastolic</sub> <sup>‡</sup>	0.03 (0.02–0.08)	0.07 (0.03–0.10)	0.03 (0.01–0.06)	0.096

CT-FFR was measured within 1 cm to the distal end of myocardial bridging.  $\Delta$ CT-FFR was measured as the difference of CT-FFR value between proximal and distal end of myocardial bridging. \*Data are mean ± standard deviation, <sup>†</sup>Data are the median, with the interquartile range in parentheses. CCTA = coronary CT angiography, FFR = fractional flow reserve

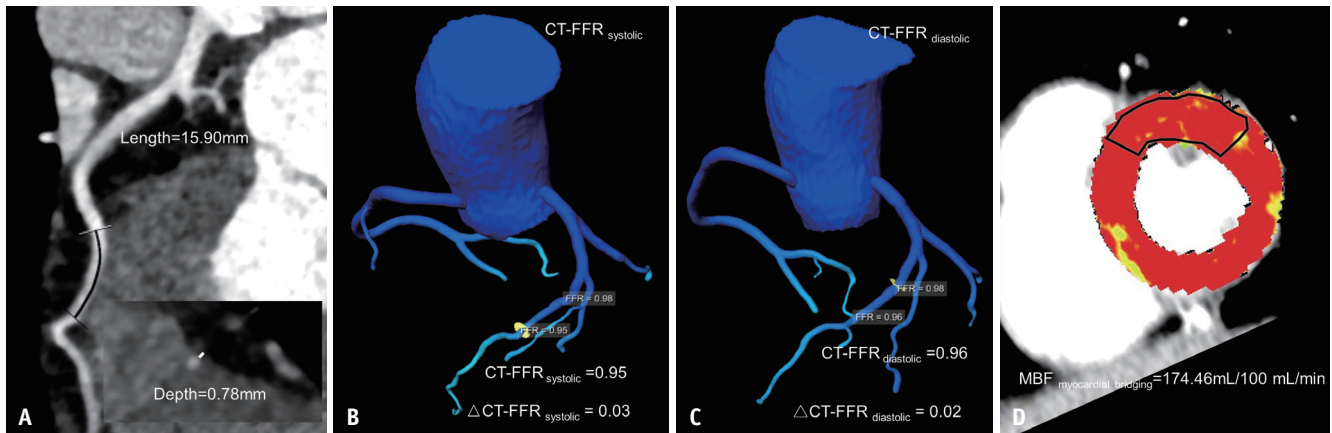


**Fig. 2. Representative case of a 54-year-old female with myocardial bridging not causing myocardial ischemia.**  
**A.** CCTA showing superficial myocardial bridging at the middle LAD, with a myocardial bridging length of 15.9 mm and a depth of 0.78 mm.  
**B.** CT-FFR<sub>systolic</sub> and  $\Delta$ CT-FFR<sub>systolic</sub> of 0.95 and 0.03, respectively. **C.** CT-FFR<sub>diastolic</sub> and  $\Delta$ CT-FFR<sub>diastolic</sub> of 0.96 and 0.02, respectively. **D.** MBF derived from dynamic CT-MPI revealing the absence of decreased myocardial perfusion of LAD territory. CCTA = coronary CT angiography, FFR = fractional flow reserve, LAD = left anterior descending artery, MBF = myocardial blood flow, MPI = myocardial perfusion imaging

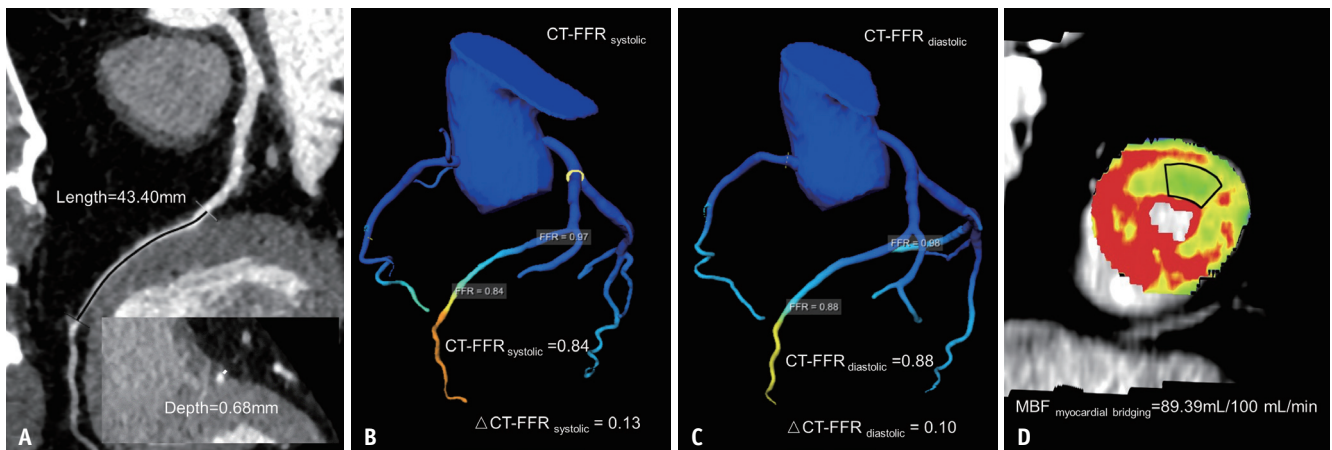


**Fig. 3. Representative case of a 67-year-old male with myocardial bridging causing myocardial ischemia.**  
**A.** CCTA showing superficial myocardial bridging at the middle LAD, with a myocardial bridging length of 43.4 mm and a depth of 0.68 mm.  
**B.** CT-FFR<sub>systolic</sub> and  $\Delta$ CT-FFR<sub>systolic</sub> of 0.84 and 0.13, respectively. **C.** CT-FFR<sub>diastolic</sub> and  $\Delta$ CT-FFR<sub>diastolic</sub> of 0.88 and 0.1, respectively. **D.** MBF derived from dynamic CT-MPI revealing decreased myocardial perfusion of the LAD territory. CCTA = coronary CT angiography, FFR = fractional flow reserve, LAD = left anterior descending artery, MBF = myocardial blood flow, MPI = myocardial perfusion imaging

specificity (85.7%, 54/63) for diagnosing myocardial bridging-related ischemia (Table 3). Nevertheless, the PPVs of CT-related parameters were low, with none exceeding 50% (Table 3).

## DISCUSSION

The major finding of the current study was that  $\Delta$ CT-FFR<sub>systolic</sub> had the highest sensitivity and NPV whereas  $\Delta$ CT-FFR<sub>diastolic</sub> had the highest specificity among all parameters for diagnosing myocardial bridging-related ischemia. In addition, the PPVs of all CT-related parameters were low.

Myocardial bridging is a congenital coronary anomaly that

can be associated with myocardial ischemia [6-8]. Functional assessment of myocardial bridging is fundamentally important for guiding treatment strategies [23]. However, owing to the unique hemodynamic characteristics of myocardial bridging during the systolic and diastolic phases, it is challenging for FFR to accurately evaluate the functional significance of myocardial bridging [24]. Unlike the hemodynamic assessment of fixed coronary stenosis, traditional FFR (average systole and diastole pressure drop) may underestimate the functional significance of myocardial bridging due to its significant diastolic pressure gradients and artificially normal or negative systolic pressure gradients [24]. Thus, diastolic FFR has been

**Table 3. Diagnostic Performance of CCTA and CT-FFR Parameters**

	AUC*	Cutoff Value	Sensitivity (%)	Specificity (%)	PPV (%)	NPV (%)	Accuracy (%)
Myocardial bridging length	0.612 (0.493–0.723)	> 32.8 mm	50.0 (6/12)	76.2 (48/63)	28.6 (6/21)	88.9 (48/54)	72.0 (54/75)
Myocardial bridging depth	0.711 (0.595–0.810)	> 0.58 mm	100 (12/12)	41.3 (26/63)	24.5 (12/49)	100 (26/26)	50.7 (38/75)
CT-FFR <sub>systolic</sub>	0.733 (0.618–0.828)	≤ 0.89	75.0 (9/12)	65.1 (41/63)	29.0 (9/31)	93.2 (41/44)	66.7 (50/75)
CT-FFR <sub>diastolic</sub>	0.623 (0.503–0.732)	≤ 0.89	75.0 (9/12)	54.0 (34/63)	23.7 (9/38)	91.9 (34/37)	57.3 (43/75)
$\Delta$ CT-FFR <sub>systolic</sub>	0.822 (0.717–0.901)	> 0.06	91.7 (11/12)	69.8 (44/63)	36.7 (11/30)	97.8 (44/45)	73.3 (55/75)
$\Delta$ CT-FFR <sub>diastolic</sub>	0.652 (0.532–0.766)	> 0.08	50.0 (6/12)	85.7 (54/63)	40.0 (6/15)	90.0 (54/60)	80.0 (60/75)

\*Values in the parentheses are 95% confidence interval. AUC = area under curve, CCTA = coronary CT angiography, FFR = fractional flow reserve, NPV = negative predictive value, PPV = positive predictive value

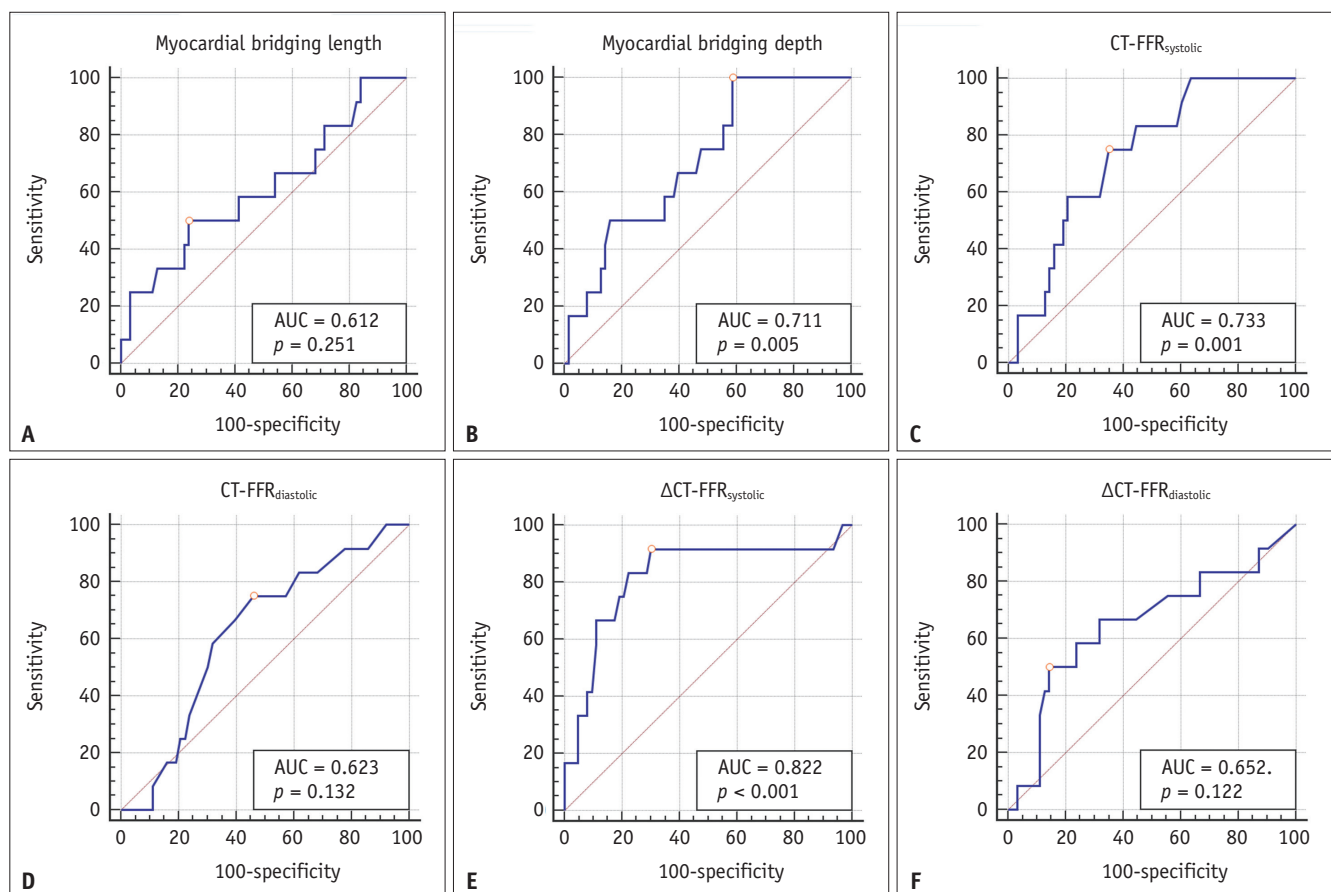


**Fig. 4. ROC analysis of myocardial bridging length, depth, CT-FFR<sub>systolic</sub>, CT-FFR<sub>diastolic</sub>,  $\Delta$ CT-FFR<sub>systolic</sub>, and  $\Delta$ CT-FFR<sub>diastolic</sub> for identifying myocardial bridging-related ischemia.**

A-F.  $\Delta$ CT-FFR<sub>systolic</sub> shows the largest AUC, followed by CT-FFR<sub>systolic</sub>, myocardial bridging depth,  $\Delta$ CT-FFR<sub>diastolic</sub>, CT-FFR<sub>diastolic</sub>, and myocardial bridging length. AUC = area under the curve, FFR = fractional flow reserve, ROC = receiver operating characteristic

recommended as a more appropriate approach for testing the hemodynamic significance of myocardial bridging [25].

Similarly, it remains unclear whether CT-FFR is feasible for the precise functional evaluation of myocardial bridging and which phase should be used for CT-FFR interpretation. To date, only one recent study explored the diagnostic

performance of CT-FFR derived from diastolic data against adenosine stress FFR [10]. The current study is the first to investigate the diagnostic accuracy of CT-FFR derived from both diastolic and systolic phases. Our findings suggested that  $\Delta$ CT-FFR<sub>systolic</sub> had the highest sensitivity whereas  $\Delta$ CT-FFR<sub>diastolic</sub> had the highest specificity for diagnosing

ischemic myocardial bridging. This result was contrary to previous studies on invasive FFR, which supported the use of diastolic FFR rather than mean FFR for the evaluation of myocardial bridging [25,26]. This discrepancy could be attributed to variations in the lumen diameter of myocardial bridging throughout the cardiac cycle. During significant systolic compression, the lumen geometry varies remarkably between phases. In this setting, the vessel lumen may have a “normal” or “mild” appearance in the diastolic phase, leading to the over-estimation of CT-FFR and low sensitivity of  $\Delta\text{CT-FFR}_{\text{diastolic}}$ . Only at the end-systolic phase does the lumen geometry represent the maximal compression. CT-FFR simulation can more closely reveal actual hemodynamic changes in myocardial bridging, resulting in the high sensitivity of  $\Delta\text{CT-FFR}_{\text{systolic}}$ .

Moreover, none of the CT-FFR parameters showed high PPV in the present study. This could be related to the limitation of the CT-FFR algorithm. The CT-FFR simulation model was developed based on the fluid dynamics of fixed tubular stenosis. However, myocardial bridging has much more complicated flow dynamics through the diastolic and systolic phases. Various factors rather than the extent of single compression are associated with the presence of myocardial ischemia of myocardial bridging. For example, tachycardia due to exercise or emotional distress reduces flow and myocardial perfusion by shortening the diastolic perfusion time and increases both epicardial coronary vasoconstriction and contraction of the myocardial bridging over the tunneled epicardial LAD [27,28]. In addition, prolongation of the myocardial bridging contraction may also cause a localized phasic coronary spasm that persists into diastole owing to a delayed relaxation time of the arterial vascular smooth muscle compared to the diastole duration, especially with tachycardia, which contributes to further worsening of coronary perfusion [29]. Thus, a functional assessment of myocardial bridging by CT-FFR simulation relying only on a single anatomical parameter (systolic compression extent) without consideration of other factors such as compression duration, diastolic filling, etc. is likely to under-estimate CT-FFR and result in a low PPV.

The current study has several clinical implications. First, because  $\Delta\text{CT-FFR}_{\text{systolic}}$  showed very high sensitivity and NPV for identifying ischemic myocardial bridging, it can be used to safely rule out hemodynamically significant myocardial bridging in routine clinical practice. However, since false-positive cases are common in CT-FFR evaluation regardless of cardiac phases used for analysis, further

functional assessment (myocardial perfusion imaging) is needed to confirm the positive results by CT-FFR. Second, the threshold of  $\Delta\text{CT-FFR}_{\text{systolic}}$  ( $> 0.06$  in the current study) to discriminate flow-limiting and non-flow limiting myocardial bridging was smaller than the conventional best cutoff ( $\geq 0.2$ , representing at least 20% of pressure drop) used for CAD evaluation. Although this value requires validation, we should be aware that the same CT-FFR threshold from CAD application cannot be used to assess myocardial bridging.

Despite the above findings, the present study has several limitations. First, all currently available CT-FFR simulation algorithms were developed to evaluate fixed luminal stenosis rather than myocardial bridging, which has more complex fluid dynamics. Although we performed separate CT-FFR analyses according to different cardiac phases (systolic and diastolic), the model was suboptimal for the assessment of myocardial bridging and had inferior diagnostic performance compared to previous CAD studies [14,30,31]. Future development of CT-FFR approaches dedicated to the evaluation of myocardial bridging is warranted to optimize the diagnostic accuracy. In addition, due to the retrospective design, the patients included in this study had stable angina and intermediate-to-high pretest probabilities of obstructive CAD. Most of the subjects showed imaging evidence of coronary atherosclerosis and, therefore, did not represent the population with isolated myocardial bridging. Finally, the limited number of positive cases and uncontrolled confounding factors reduced the generalizability of the results of the present study. While the overall incidence of myocardial bridging-related ischemia was low in clinical practice [32], the small proportion of patients with functionally significant myocardial bridging undermined the statistical power of the current analysis. Further studies with more subjects are needed.

In conclusion,  $\Delta\text{CT-FFR}_{\text{systolic}}$  reliably excluded myocardial bridging-related ischemia with high sensitivity and NPV. Myocardial bridging showing positive CT-FFR results requires further evaluation with other functional imaging modalities.

## Supplement

The Supplement is available with this article at <https://doi.org/10.3348/kjr.2021.0043>.

## Conflicts of Interest

The authors have no potential conflicts of interest to

disclose.

### Author Contributions

Conceptualization: Jiayin Zhang. Data curation: Yarong Yu, Jiayin Zhang. Formal analysis: Yarong Yu, Jiayin Zhang. Funding acquisition: Jiayin Zhang. Investigation: Yarong Yu, Lihua Yu. Methodology: Yarong Yu, Xu Dai. Project administration: Jiayin Zhang. Resources: Jiayin Zhang. Software: Yarong Yu. Supervision: Jiayin Zhang. Validation: Lihua Yu. Writing—original draft: Jiayin Zhang, Yarong Yu. Weiting—review & editing: Jiayin Zhang.

### ORCID iDs

Yarong Yu

<https://orcid.org/0000-0002-8752-3159>

Lihua Yu

<https://orcid.org/0000-0003-0586-3780>

Xu Dai

<https://orcid.org/0000-0002-7487-6713>

Jiayin Zhang

<https://orcid.org/0000-0001-7383-7571>

### REFERENCES

- Kim PJ, Hur G, Kim SY, Namgung J, Hong SW, Kim YH, et al. Frequency of myocardial bridges and dynamic compression of epicardial coronary arteries: a comparison between computed tomography and invasive coronary angiography. *Circulation* 2009;119:1408-1416
- Leschka S, Koepfli P, Husmann L, Plass A, Vachenaer R, Gaemperli O, et al. Myocardial bridging: depiction rate and morphology at CT coronary angiography--comparison with conventional coronary angiography. *Radiology* 2008;246:754-762
- Yu M, Zhang Y, Li Y, Li M, Li W, Zhang J. Assessment of myocardial bridge by cardiac CT: intracoronary transluminal attenuation gradient derived from diastolic phase predicts systolic compression. *Korean J Radiol* 2017;18:655-663
- Li Y, Yu M, Zhang J, Li M, Lu Z, Wei M. Non-invasive imaging of myocardial bridge by coronary computed tomography angiography: the value of transluminal attenuation gradient to predict significant dynamic compression. *Eur Radiol* 2017;27:1971-1979
- Möhlenkamp S, Hort W, Ge J, Erbel R. Update on myocardial bridging. *Circulation* 2002;106:2616-2622
- Ural E, Bildirici U, Celikyurt U, Kilic T, Sahin T, Acar E, et al. Long-term prognosis of non-interventionally followed patients with isolated myocardial bridge and severe systolic compression of the left anterior descending coronary artery. *Clin Cardiol* 2009;32:454-457
- Kodama K, Morioka N, Hara Y, Shigematsu Y, Hamada M, Hiwada K. Coronary vasospasm at the site of myocardial bridge--report of two cases. *Angiology* 1998;49:659-663
- Tio RA, Van Gelder IC, Boonstra PW, Crijns HJ. Myocardial bridging in a survivor of sudden cardiac near-death: role of intracoronary doppler flow measurements and angiography during dobutamine stress in the clinical evaluation. *Heart* 1997;77:280-282
- Tarantini G, Migliore F, Cademartiri F, Fraccaro C, Iliceto S. Left anterior descending artery myocardial bridging: a clinical approach. *J Am Coll Cardiol* 2016;68:2887-2899
- Zhou F, Wang YN, Schoepf UJ, Tesche C, Tang CX, Zhou CS, et al. Diagnostic performance of machine learning based CT-FFR in detecting ischemia in myocardial bridging and concomitant proximal atherosclerotic disease. *Can J Cardiol* 2019;35:1523-1533
- Bamberg F, Marcus RP, Becker A, Hildebrandt K, Bauner K, Schwarz F, et al. Dynamic myocardial CT perfusion imaging for evaluation of myocardial ischemia as determined by MR imaging. *JACC Cardiovasc Imaging* 2014;7:267-277
- Ho KT, Chua KC, Klotz E, Panknin C. Stress and rest dynamic myocardial perfusion imaging by evaluation of complete time-attenuation curves with dual-source CT. *JACC Cardiovasc Imaging* 2010;3:811-820
- Yang J, Dou G, He B, Jin Q, Chen Z, Jing J, et al. Stress myocardial blood flow ratio by dynamic CT perfusion identifies hemodynamically significant CAD. *JACC Cardiovasc Imaging* 2020;13:966-976
- Li Y, Yu M, Dai X, Lu Z, Shen C, Wang Y, et al. Detection of hemodynamically significant coronary stenosis: CT myocardial perfusion versus machine learning CT fractional flow reserve. *Radiology* 2019;293:305-314
- Li Y, Dai X, Lu Z, Shen C, Zhang J. Diagnostic performance of quantitative, semi-quantitative, and visual analysis of dynamic CT myocardial perfusion imaging: a validation study with invasive fractional flow reserve. *Eur Radiol* 2021;31:525-534
- Schwarz F, Hinkel R, Baloch E, Marcus RP, Hildebrandt K, Sandner TA, et al. Myocardial CT perfusion imaging in a large animal model: comparison of dynamic versus single-phase acquisitions. *JACC Cardiovasc Imaging* 2013;6:1229-1238
- Hubbard L, Lipinski J, Ziemer B, Malkasian S, Sadeghi B, Javan H, et al. Comprehensive assessment of coronary artery disease by using first-pass analysis dynamic CT perfusion: validation in a swine model. *Radiology* 2018;286:93-102
- Itu L, Rapaka S, Passerini T, Georgescu B, Schwemmer C, Schoebinger M, et al. A machine-learning approach for computation of fractional flow reserve from coronary computed tomography. *J Appl Physiol (1985)* 2016;121:42-52
- Yu M, Dai X, Yu L, Lu Z, Shen C, Tao X, et al. Hemodynamic change of coronary atherosclerotic plaque after statin treatment: a serial follow-up study by computed tomography-derived fractional flow reserve. *J Am Heart Assoc* 2020;9:e015772

20. Bamberg F, Klotz E, Flohr T, Becker A, Becker CR, Schmidt B, et al. Dynamic myocardial stress perfusion imaging using fast dual-source CT with alternating table positions: initial experience. *Eur Radiol* 2010;20:1168-1173
21. Cerqueira MD, Weissman NJ, Dilsizian V, Jacobs AK, Kaul S, Laskey WK, et al. Standardized myocardial segmentation and nomenclature for tomographic imaging of the heart. A statement for healthcare professionals from the Cardiac Imaging Committee of the Council on Clinical Cardiology of the American Heart Association. *Circulation* 2002;105:539-542
22. Tonino PA, Fearon WF, De Bruyne B, Oldroyd KG, Leesar MA, Ver Lee PN, et al. Angiographic versus functional severity of coronary artery stenoses in the FAME study fractional flow reserve versus angiography in multivessel evaluation. *J Am Coll Cardiol* 2010;55:2816-2821
23. Schwarz ER, Gupta R, Haager PK, vom Dahl J, Klues HG, Minartz J, et al. Myocardial bridging in absence of coronary artery disease: proposal of a new classification based on clinical-angiographic data and long-term follow-up. *Cardiology* 2009;112:13-21
24. Hakeem A, Cilingiroglu M, Leesar MA. Hemodynamic and intravascular ultrasound assessment of myocardial bridging: fractional flow reserve paradox with dobutamine versus adenosine. *Catheter Cardiovasc Interv* 2010;75:229-236
25. Escaned J, Cortés J, Flores A, Goicolea J, Alfonso F, Hernández R, et al. Importance of diastolic fractional flow reserve and dobutamine challenge in physiologic assessment of myocardial bridging. *J Am Coll Cardiol* 2003;42:226-233
26. Sen S, Asrress KN, Nijjer S, Petraco R, Malik IS, Foale RA, et al. Diagnostic classification of the instantaneous wave-free ratio is equivalent to fractional flow reserve and is not improved with adenosine administration. Results of CLARIFY (Classification Accuracy of Pressure-Only Ratios Against Indices Using Flow Study). *J Am Coll Cardiol* 2013;61:1409-1420
27. Bourassa MG, Butnaru A, Lespérance J, Tardif JC. Symptomatic myocardial bridges: overview of ischemic mechanisms and current diagnostic and treatment strategies. *J Am Coll Cardiol* 2003;41:351-359
28. Gould KL, Johnson NP. Imaging coronary blood flow in AS: let the data talk, again. *J Am Coll Cardiol* 2016;67:1423-1426
29. Gould KL, Johnson NP. Myocardial bridges: lessons in clinical coronary pathophysiology. *JACC Cardiovasc Imaging* 2015;8:705-709
30. Li Z, Zhang J, Xu L, Yang W, Li G, Ding D, et al. Diagnostic accuracy of a fast computational approach to derive fractional flow reserve from coronary CT angiography. *JACC Cardiovasc Imaging* 2020;13:172-175
31. Yu M, Lu Z, Shen C, Yan J, Wang Y, Lu B, et al. The best predictor of ischemic coronary stenosis: subtended myocardial volume, machine learning-based FFRCT, or high-risk plaque features? *Eur Radiol* 2019;29:3647-3657
32. Uusitalo V, Saraste A, Pietilä M, Kajander S, Bax JJ, Knuuti J. The functional effects of intramural course of coronary arteries and its relation to coronary atherosclerosis. *JACC Cardiovasc Imaging* 2015;8:697-704